Nonlinear feedback control of Quadrotors exploiting First-Order Drag Effects

Jean-Marie Kai, Guillaume Allibert, Minh-Duc Hua, Tarek Hamel

Nonlinear feedback control of Quadrotors exploiting First-Order Drag Effects

Jean-Marie Kai * **Guillaume Allibert** * **Minh-Duc Hua** *
Tarek Hamel *

* *Université Côte d'Azur, CNRS, I3S, France*
(e-mails: kai@i3s.unice.fr, allibert@i3s.unice.fr, hua@i3s.unice.fr, thamel@i3s.unice.fr).

Abstract: We exploit the first-order aerodynamic effects for the feedback control of quadrotors in order to enhance the performance of the closed-loop system. We describe first the origin of these forces and then we show how the complexity of the system dynamics can be transformed by a change of control input into a simpler form, for which the classical hierarchical control approach (slightly modified here) can be applied. The simulation results illustrate the soundness of the proposed drag-augmented control scheme.

Keywords: UAVs, Lyapunov methods, Application of nonlinear analysis and design, Guidance navigation and control, Modeling for control, Nonlinear control.

1. INTRODUCTION

Quadrotors have become one of the most popular configurations for aerial robotics, this is due to their particular underactuated and unstable dynamics that were studied extensively by the control and robotics research communities. Their development was primarly boosted by the advancement and the drop in price of sensors and batteries technologies. This is without mentioning their numerous applications that are increasingly commercialized.

In classical studies of miniature multi-rotor helicopters Hamel et al. (2002), the rotor blades are assumed to be rigid and considered to be producing a thrust force along the direction of the shaft, a resisting torque as well as a gyroscopic torque due to the tendency of the rotors to preserve their direction of rotation. In Pounds (2007), the blades are considered to be able to pivot around a hinge in analogy with helicopters' rotors where in this case the gyroscopic torque is not transmitted entirely to the body of the rotorcraft. This in turn however generates the flapping phenomenon that complexifies the modeling of the aerodynamic forces. In Bristeau et al. (2009), Pounds et al. (2010), Bangura and Mahony (2012), Mahony et al. (2012) and Bangura et al. (2016), it has been considered that due to the natural flexibility of the blades, small-scale hingeless rotors exhibit similar mechanical behavior to the one produced by hinged rotors and hence more accurate modeling of their aerodynamics can be inspired from the rich literature on helicopter dynamics, see Prouty (2002), Bramwell (2001). The flapping dynamics were exploited mainly for designing velocity estimators. In Martin and Salaun (2010), the authors showed that around hovering flight the first order aerodynamic drag due to the propellers injects information about the vehicle's velocity in the accelerometer measurements. As for the control design, these drag forces are often neglected, except in some few studies. In Pounds et al. (2010); Martin and Salaun (2010) and Plessis and Pounds (2014) linear control techniques were developed for hovering flight conditions, taking into account these drag forces only for attitude control purposes. To the authors' knowledge, the first nonlinear control dealing with the full dynamics of the system has been presented in Omari et al. (2013) by exploiting a hierarchical control methodology, however the drag model that was proposed is a rough approximation.

In this paper we revisit the modeling of the first-order drag by explaining the physical origins of the phenomenon, then we express mathematically these forces in case of rigid as well as flexible rotor blades and apply them to the case of a quadrotor (Sect. 2). Then inspired by the works in Omari et al. (2013) we explain how a part of these forces can be compensated for in the position controller design by decomposing the aerodynamic forces vector into a component that is independent of the vehicle's orientation and another component along the thrust direction allowing us to define an explicit desired orientation for the orientation control loop. In order to address also the problem of ignored dynamics we propose to add a bounded integrator, complemented with anti-windup capabilities, that improves the convergence to the desired trajectory (Sect. 3). The control methodology is analyzed in simulation and finally results are presented and commented (Sect. 4).

2. DYNAMIC MODEL OF A VTOL

Let $\mathcal{I} = \{e_1^{\mathcal{I}}, e_2^{\mathcal{I}}, e_3^{\mathcal{I}}\}$ denote a right-hand inertial frame stationary with respect to the earth and such that $e_3^{\mathcal{I}}$ denotes the vertical direction downwards into the earth. Let the vector $\xi = (x, y, z)$ denote the position of the centre of mass of the object in the frame $\mathcal{I}$ relative to a fixed origin $O \in \mathcal{I}$. Let $\mathcal{B} = \{e_1^{\mathcal{B}}, e_2^{\mathcal{B}}, e_3^{\mathcal{B}}\}$ be a body-fixed frame whose center coincides with the center of mass of the vehicle and such that $e_3^{\mathcal{B}}$ is in the opposite direction of thrust generation. The attitude of the body-fixed frame is represented by a rotation matrix, element of the Special

Orthogonal group $SO(3)$, $R \in SO(3) : \mathcal{B} \to \mathcal{I}$. We use $\{e_1, e_2, e_3\}$ for the canonical basis in $\mathbb{R}^3$.

Let $\Omega \in \mathcal{B}$ be the vector of coordinates of the angular velocity of the vehicle with respect to $\mathcal{I}$. Let $v \in \mathcal{I}$ and $v_a = v - v_w \in \mathcal{I}$ denote respectively the vectors of coordinates of the vehicle's velocity and air-velocity with respect to $\mathcal{I}$. Let m be the overall mass of the vehicle and $I \in \mathbb{R}^{3\times3}$ its fixed inertia matrix with respect to $\mathcal{B}$. Suppose that the vehicle is equipped with N identical rotors each of which producing a thrust in the opposite direction of $e_3^{\mathcal{B}}$. The angular velocity of each rotor with respect to $\mathcal{B}$ is denoted by $\omega_i e_3^{\mathcal{B}}$, and its inertia with respect to $\mathcal{B}$ is denoted by $J = J_i \in \mathbb{R}^{3\times3}$. For any vector of coordinates $u \in \mathbb{R}^3$, $\pi_{e_3} u$ represents its projection on the plane (e_1, e_2) along e_3, i.e. $\pi_{e_3} = I - e_3 e_3^\top$.

Applying the Newton-Euler formalism to the system, one gets for translational and rotational kinematics:

$$\dot{\xi} = v \tag{1}$$

$$\dot{R} = R\Omega_\times \tag{2}$$

where $\Omega_\times$ is the skew symmetric matrix associated with vector Ω, such that $\Omega_\times u = \Omega \times u$ for any vector $u \in \mathbb{R}^3$. Then for translational, and rotational dynamics:

$$m\dot{v} = mge_3 - TRe_3 + RF_a \tag{3}$$

$$I\dot{\Omega} = -\Omega_\times I\Omega + \tau_g + \tau + \tau_a \tag{4}$$

where mge_3 is the total weight, $T \in \mathbb{R}^+$ is the collective thrust generated by the N rotors and represents the first control input, $\tau \in \mathbb{R}^3$ is the torque vector expressed in $\mathcal{B}$ and constitutes the second control input; it is directly generated by the thrusts of the N rotors. The term $F_a \in \mathcal{B}$ represents the body drag and parasitic aerodynamic forces due to the thrust generation and the vehicle motion, $\tau_g \in \mathcal{B}$ represents gyroscopic torques due to the interaction of rotating rotors with the body of the vehicle and finally, $\tau_a \in \mathcal{B}$ represents the remaining parasitic aerodynamic torques.

In the following subsections, we further develop the terms F_a, τ_a and τ_g that depend linearly on the velocity, according to the assumptions made on the propellers' characteristics and mounting. However, we will neglect second order aerodynamic forces. This is a reasonable assumption for the dynamics of a UAV in quasi-stationary flight where the exogenous aerodynamical forces depending on the square of the linear velocity are negligible.

2.1 Classical rigid rotors:

By rigid we are considering that the only allowed motion for a blade is its rotation around the corresponding shaft.

According to the law of momentum conservation, when each rigid propeller is rotating with an angular speed ω_i with respect to the vehicle whose angular velocity is Ω, the gyroscopic torque applied on the vehicle by all the N rotors is given by:

$$\tau_g = -\sum_{i=1}^{N} \Omega \times J_i \omega_i e_3 = -J \sum_{i=1}^{N} \Omega \times \omega_i e_3. \tag{5}$$

From the classical aerodynamics, the thrust generated by a rotor in hovering conditions is proportional to the square of a rotor's angular speed and hence the total generated thrust is given by $T = \sum_{i=1}^{N} T_i$ where $T_i = c_T \omega_i^2$ is the thrust produced by the i^{th} rotor (c_T is a positive constant). When the rotor is moving in a certain direction, the advancing blade produces a higher relative air-velocity than that produced by the retreating blade and therefore the magnitude of aerodynamic forces, that depend on the air-velocity, will be higher on the advancing blade. This difference leads to nonzero net forces and torques on the vehicle. The parasitic force resulting from the drag components lies in the horizontal plane of the rotor. It is called H-Force in the specialized literature and can be expressed (see for instance Prouty (2002), Martin and Salaun (2010)) by:

$$F_a = \sum_{i=1}^{N} F_{drag}^i = \sum_{i=1}^{N} -\sqrt{T_i} c_{d1} \pi_{e_3} V_a^i \tag{6}$$

where c_{d1} is a positive constant, and $V_a^i = R^T v_a + \Omega \times d_i$ is the translational air-velocity of the i^{th} rotor expressed in the vehicle's body-fixed frame, with d_i the position of the i^{th} rotor with respect to the center of mass of the vehicle. Note that F_a is a first-order drag since it is directly proportional to the airspeed.

As for the parasitic torque τ_a, it can be written as a combination of a pure torque created by the difference between the lift forces of the advancing and retreating blades, a drag damping effect, and the torques created by the forces F_{drag}^i (6). It can be expressed as follows:

$$\tau_a = \sum_{i=1}^{N} -\mathrm{sgn}(\omega_i)\sqrt{T_i} c_{d2} \pi_{e_3} V_a^i - \sqrt{T_i} c_{d3} \pi_{e_3} \Omega + d_i \times F_{drag}^i \tag{7}$$

where c_{d2} and c_{d3} are positive constants.

Finally, the control term τ is composed of the torques produced by the thrust forces $-T_i e_3$ as well as the drag torques around the shafts of the motors. It can be expressed as:

$$\boldsymbol{\tau} = \sum_{i=1}^{N} -d_i \times T_i e_3 + \sum_{i=1}^{N} -\mathrm{sgn}(\omega_i) c_Q \omega_i^2 e_3 \tag{8}$$

with c_Q a positive constant.

2.2 Flexible rotors:

Most rotor blades are not completely rigid due to their elastic bending properties, and are flexible enough to reduce the gyroscopic effects as well as the pure aerodynamical torques that appeared in the rigid case. This comes at the expense of an additional "flapping" term in the expression of the aerodynamic force F_a which becomes of the form:

$$F_a = \sum_{i=1}^{N} (F_{flap}^i + F_{drag}^i) \tag{9}$$

where F_{drag}^i is expressed by (6) and it is always present in the flexible case.

In Prouty (2002), Bramwell (2001), it is shown that a hingeless rotor is equivalent to a hinged rotor with a nonzero offset from the shaft depending on its flexibility and therefore it will exhibit similar aerodynamic effects specially for small rotation around the "virtual hinge" where aerodynamic and coriolis forces overcome any elastic force of the material.

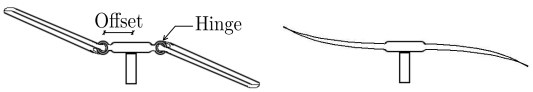

Fig. 1. Hinged (left) and hingeless (right) blades

Complete studies of hinged rotor's mechanisms can be found in Prouty (2002) and Bramwell (2001). In this paper we will only focus on describing the phenomenon qualitatively and present modeling solutions suitable for control purposes. In the following the term hinge can refer to an actual hinge or a virtual one for the case of hingeless rotors. During rotation of the shaft, the blade is subject to a number of forces creating torques around the hinge, thus a rotation around the hinge is added to its rotation around the shaft. An equilibrium will be attained when the blades remain in a plane (not necessarily normal to the shaft) called the "tip path plane" causing tilting of the thrust direction.

This phenomenon can be explained by starting from the case of rigid blades, where the same torques resulting from the difference in lift forces between the advancing and retreating blade, instead of directly being transmitted to the vehicle are absorbed by the blades that can now flap around their hinges. It is shown that as a final effect the tip path plane tilts away from the apparent wind caused by the translational motion.

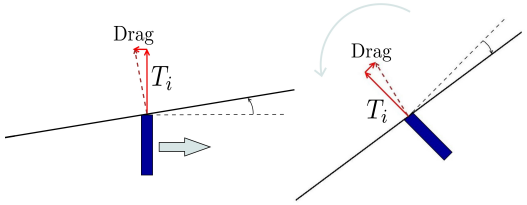

Fig. 2. Translational (left) and Rotational (right) flapping

The same reasoning applies for the tendency of gyroscopic torques to preserve the orientation of the rotating blades, once again they are not transmitted to the vehicle anymore. However, they contribute to the flapping motion of the blades around their hinges leading to a negligible gyroscopic effect ($\tau_g \simeq 0$).

The direction of the total thrust force is approximately normal to the tip path plane resulting from the flapping whereas the accepted model of the total flapping force F^i_{flap} generated by the i^{th} rotor can be expressed as follows (see Prouty (2002) and Martin and Salaun (2010) for more details):

$$\begin{aligned} F^i_{flap} = &-\sqrt{T_i}c_{av}\pi_{e_3}V^i_a + \mathrm{sgn}(\omega_i)\sqrt{T_i}c_{bv}\ e_3 \times V^i_a \\ &- \mathrm{sgn}(\omega_i)\sqrt{T_i}c_{b\Omega}\pi_{e_3}\Omega - \sqrt{T_i}c_{a\Omega}\ e_3 \times \Omega \end{aligned} \tag{10}$$

where $c_{av}, c_{bv}, c_{a\Omega}$ and $c_{b\Omega}$ are positive constants depending on aerodynamic coefficients and geometry of the blades. In addition to altering the direction of thrust, flapping induces a pure torque around the hubs of hinges as explained in Prouty (2002). For simplicity, this hub torque is lumped into the existing ones and without loss of generality the parasitic torque $\boldsymbol{\tau_a}$ can be expressed as:

$$\tau_a = \sum_{i=1}^{N} d_i \times (F^i_{flap} + F^i_{drag}) \tag{11}$$

Finally the expression of the control term τ in equation (8) remains the same.

2.3 Application to the Quadrotor:

Consider a quadrotor with the configuration shown in figure (3). The positions of the centers of the rotors are referred to by the vectors: $d_1 = (d, 0, -e)^\top$, $d_2 = (0, -d, -e)^\top$, $d_3 = (-d, 0, -e)^\top$ and $d_4 = (0, d, -e)^\top$, where $d > 0$, and e can be positive if the rotors are above the center of mass of the vehicle or negative if they are below the center of mass. The rotors are chosen to be rotating in opposite directions such that $\omega_1 > 0, \omega_2 < 0, \omega_3 > 0$ and $\omega_4 < 0$. According to the previous sections,

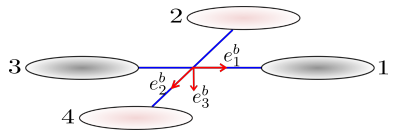

Fig. 3. Quadrotor configuration

we can sum the aerodynamic forces created by all the four rotors and get the expressions for the quadrotor model. This will lead to a complex dynamic system suitable for simulations. For control purposes, it is however crucial to elaborate a simpler dynamic system based on realistic assumptions (fulfilled in first approximation), for which classical nonlinear control methodologies apply. This can be done by considering that quadrotors operate near hover conditions where the thrust generated by the rotors compensate together the overall weight of the vehicle, so that $\sqrt{T_i}$ in the expressions (6), (7) and (10) can be approximated by $\sqrt{mg/4}\ \forall i$.

Since almost all existing quadrotors are equipped with nonrigid hingeless rotors, Newton's equations of motion for a typical quadrotor subject to the forces and torques outlined above are:

$$\dot{\xi} = v \tag{12}$$

$$m\dot{v} = mge_3 - TRe_3 - RAR^\top v_a - RB\Omega \tag{13}$$

$$\dot{R} = R\Omega_\times \tag{14}$$

$$I\dot{\Omega} = -\Omega_\times I\Omega - \tau^r_g + \tau - CR^\top v_a - D\Omega \tag{15}$$

with, $A = a_{11}\pi_{e3}$, $B = b_{12}e_{3\times}$, $C = -c_{12}e_{3\times}$, and $D = d_{11}\pi_{e3} + d_{33}e_3e_3^T$, where $a_{11} = 2\sqrt{mg}(c_{d1} + c_{av})$, $b_{12} = 2\sqrt{mg}(c_{a\Omega} + ec_a)$, $c_{12} = 2e\sqrt{mg}(c_{av} + c_{d1})$, $d_{11} = 2\sqrt{mg}(e^2(c_{av} + c_{d1}) + ec_{a\Omega})$ and $d_{33} = 2d^2\sqrt{mg}\ (c_{av} + c_{d1})$ are positive constants and τ^r_g the residual gyroscopic effect. Finally, the net force and moments produced by the rotors and used as control inputs are:

$$\begin{pmatrix} T \\ \tau \end{pmatrix} = \begin{pmatrix} c_T & c_T & c_T & c_T \\ 0 & -dc_T & 0 & dc_T \\ dc_T & 0 & -dc_T & 0 \\ -c_Q & c_Q & -c_Q & c_Q \end{pmatrix} \begin{pmatrix} \omega_1^2 \\ \omega_2^2 \\ \omega_3^2 \\ \omega_4^2 \end{pmatrix}. \tag{16}$$

By inverting equation (16), we get the rotor's desired angular speeds assumed here that they are able to generate simultaneously and instantaneously a desired torque vector τ and a desired positive thrust T. This model requires some additional comments and remarks:

(1) Using the assumption that $\sqrt{T_i} \simeq \sqrt{mg/4}$ in the expressions (6), (7) and (10), the terms involving $\text{sgn}(\omega_i)$ cancel each other out and hence they do not appear in the above model.
(2) It is straightforward to verify that the main differences between a quadrotor equipped with rigid and another equipped with flexible blades lie in the fact that the blade's flexibility reduces gyroscopic torques (τ_g^r is a residual effect) at the expense of increasing the first-order drag forces and adding a 'small' dependency of these forces on the vehicle's angular velocity ($B \neq 0$).
(3) The flexible nature of the blades typically used in practice makes the distinction between the flapping and drag parameters hopeless. Therefore, it seems reasonable to directly consider the lumped parameters a_{11}, b_{12}, c_{12}, d_{11} and d_{33}. Unlike the translational forces, aerodynamical torques as well as residual gyroscopic effects are of less interest. This is due to the full actuation of the rotational dynamics (15), that ensures a quick exponential convergence of the angular velocity Ω to any bounded desired value Ω_d. Indeed we can apply any control of the form:

$$\tau = -k_\Omega(\Omega - \Omega_d) + \Omega_\times I\Omega_d + I\dot{\Omega}_d \qquad (17)$$

where parasitic gyroscopic torques, and torques caused by the flapping and drag forces, are counteracted by a sufficiently large gain k_Ω.

The remaining part of the system, given by Equations (12)-(14) with T and Ω as control inputs, is difficult to control due to the presence of the flapping force part that depends on Ω ($B \neq 0$). This part of the flapping force is typically small and therefore an approximate model, in which this term is set to zero ($B = 0$) (basically the quadrotor is regarded as equipped with rigid rotors), is used in the control design. However, when a controller designed for the approximate system is applied to the system dynamics (12)-(14) (in presence of flapping) one can expect some loss of performance. The goal of the next section is to provide an analysis of the robustness of a controller designed in this manner by exploiting the main aerodynamical forces classically ignored in the control design and leave, for a less complicated presentation, further discussion on the dynamic perturbation ($B \neq 0$) to simulation (Sect. 4).

3. CONTROL DESIGN FOR THE QUADROTOR

We have chosen to use a hierarchical control design in order to exploit the natural robustness and practical implementation of such methodology Hua et al. (2013) described here by figure 4. The underactuated translational system is controlled by the thrust direction and magnitude through the term TRe_3. This constitutes a high-level outer loop for the control design. The desired attitude can then be reached by considering the body's angular velocity Ω as an intermediary control input, which constitutes again a desired angular velocity for the fully actuated orientation dynamics via the high gain control torque τ (17). The so-called induced and flapping drag force $-RAR^\top v_a$ in equation (13) is typically neglected in nonlinear control design of quadrotors. This is particularly due to its dependence on the orientation that prevents the definition of the desired direction of the thrust. The induced and flapping

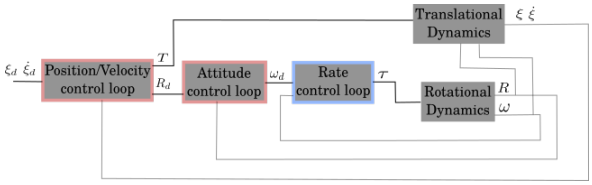

Fig. 4. Control Architecture

drag force, is not a pure drag (i.e. a dissipative force) for the quadrotor that essentially contributes to the system's stability as commonly thought. The control methodology here exploited is an application (slightly modified) of the work described in Pucci et al. (2015); Omari et al. (2013). In particular we show that the seemingly difficult problem of controlling the system (12)-(14), with $B = 0$ can be transformed into a simpler one. The key idea consists in decomposing the external force $-RAR^\top v_a$ into two components, one which is independent of the vehicle's attitude (a pure dissipative drag term), and the other along the thrust direction, this will lead to an explicit expression for the desired thrust direction (see Fig. (5)). This is of course different from the classical decomposition of the aerodynamic force to a drag component in the opposite direction of the air velocity and a lift component orthogonal to the air velocity. The above discussion can be formalized as

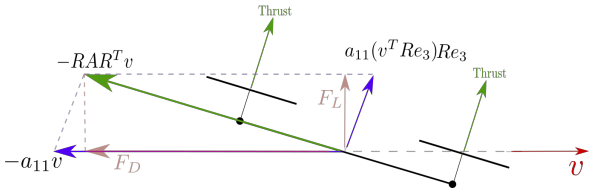

Fig. 5. Drag force decomposition

follows. Let ξ_r be the desired trajectory of the center of mass. Let $\tilde{\xi} = \xi - \xi_r$ and $\dot{\tilde{\xi}} = \dot{\xi} - \dot{\xi}_r$ be the errors on position and velocity tracking. Let us neglect the presence of wind ($v_a = \dot{\xi}$) for the moment. Differentiating $\dot{\tilde{\xi}}$, recalling (13) and decomposing the induced and flapping drag force into a component in the direction $\dot{\xi}$ and a component in the direction Re_3, it yields:

$$\ddot{\tilde{\xi}} = -\ddot{\xi}_r + ge_3 - \frac{a_{11}}{m}\dot{\tilde{\xi}} - \frac{a_{11}}{m}\dot{\xi}_r - \frac{1}{m}(T - a_{11}(\dot{\xi}^\top Re_3))Re_3. \qquad (18)$$

Let $h(\tilde{\xi}, \dot{\tilde{\xi}})$ (with $h(0,0) = 0$) be a bounded feedback term, define $\gamma_e = -h(\tilde{\xi}, \dot{\tilde{\xi}}) - \ddot{\xi}_r + ge_3 - \frac{a_{11}}{m}\dot{\xi}_r$, a term that does not depend on the orientation of the vehicle, and $\bar{T} = T - a_{11}(\dot{\xi}^\top Re_3)$. Equation (18) becomes,

$$\ddot{\tilde{\xi}} = h(\tilde{\xi}, \dot{\tilde{\xi}}) - \frac{a_{11}}{m}\dot{\tilde{\xi}} + \gamma_e - \frac{1}{m}\bar{T}Re_3. \qquad (19)$$

By imposing the following dynamics of $\dot{\tilde{\xi}}$: $\ddot{\tilde{\xi}} = h(\tilde{\xi}, \dot{\tilde{\xi}}) - \frac{a_{11}}{m}\dot{\tilde{\xi}}$ and choosing $h(\tilde{\xi}, \dot{\tilde{\xi}})$ that ensures the asymptotic stabilization of the translational dynamics to the equilibrium $(\tilde{\xi}, \dot{\tilde{\xi}}) = (0,0)$, it follows that $\gamma_e - \frac{1}{m}\bar{T}Re_3 = 0$. This in turn implies that:

(1) $\bar{T} = m\gamma_e^T Re_3$ and hence $T = \bar{T} + a_{11}(\dot{\xi}^\top Re_3)$. Using the fact that T should be positive, one can impose:

$$T = \max\left(m\gamma_e^\top Re_3 + a_{11}\dot{\xi}^\top Re_3, 0\right) \quad (20)$$
$$= \max\left(m\left(-h - \ddot{\xi}_r + ge_3 + \frac{a_{11}}{m}\dot{\xi}\right)^\top Re_3, 0\right)$$

(2) $\eta = Re_3$, the thrust direction, should converge instantaneously to:
$$\eta_d = \gamma_e/|\gamma_e|. \quad (21)$$
By instantaneously we mean a time scale separation between the attitude and linear dynamics of the airframe is required in order to be able to neglect the convergence effect of η to η_d.

To ensure that γ_e does not vanish to avoid any singularity in specifying the desired attitude it should be sufficient to choose the reference trajectory with not too strong acceleration with respect to the gravity and also to saturate $h(\tilde{\xi}, \dot{\tilde{\xi}})$ below a certain value such that $(|h(\tilde{\xi}, \dot{\tilde{\xi}})| + |\ddot{\xi}_r| < g))$ [1]. The feedback controller $h(\tilde{\xi}, \dot{\tilde{\xi}})$ can be designed as a nonlinear saturated PD controller, as follows:

$$h(\tilde{\xi}, \dot{\tilde{\xi}}) = -\text{sat}_{\Delta^p}(k^p\tilde{\xi}) - \text{sat}_{\Delta^v}(k^v\dot{\tilde{\xi}}) \quad (22)$$

where $\text{sat}_\Delta(x) = x\min(1, \Delta/|x|)$ is the classical saturation function, with Δ a positive number, and k^p, k^v positive gains. The next step consists in the computation of the desired angular velocity Ω_d involved in the inner-loop (17) that stabilizes the thrust direction η to the desired vector η_d. It is straightforward to verify that only the first two components of the desired angular velocity $\Omega_d^{1,2}$ are involved while the third component Ω_d^3 can be used freely for the control of the yaw motion.

One of many possibilities is the following choice (Pucci et al. (2015)):

$$\Omega_d = R^T((k_1(\eta, t) + \frac{\dot{\gamma}(t)}{\gamma(t)})\ \eta \times \eta_d + \Omega_{ff} + \lambda(\eta, t)\eta), \quad (23)$$

Which ensures the exponential stability of the equilibrium $\eta = \eta_d$, provided that $\eta(0) \neq -\eta_d(0)$. The term $\Omega_{ff} = \eta_d \times \dot{\eta}_d$ represents a feedforward term, $\lambda(.)$ can be any real-valued continuous function representing the free degree of freedom of yaw control, $\gamma(.)$ any smooth positive real-valued function, and $k_1(.)$ any continuous positive real-valued function.

The stability proof of the proposed controller follows the same lines of the proof proposed in Pucci et al. (2015). Consider the following candidate Lyapunov function:

$$V_1 = \frac{\gamma^2(t)}{2}\frac{1 - \eta\cdot\eta_d}{1 + \eta\cdot\eta_d} = \frac{\gamma^2(t)}{2}\frac{|\eta \times \eta_d|^2}{(1 + \eta\cdot\eta_d)^2}. \quad (24)$$

Differentiating V_1 with respect to time and recalling (23), one gets:

$$\dot{V}_1 = -2k_1(\eta, t)V_1. \quad (25)$$

This shows that V_1 converges exponentially to zero.

In order to prove the asymptotic stability of the whole system defined by (12)-(14) in case where $B = 0$ to the equilibrium $(\xi, v, \eta) = (\xi_r, v_r, \eta_d)$, we recall equation (19), and use the fact that $\gamma_e = |\gamma_e|\eta_d$ and $\bar{T} = m\gamma_e^\top\eta = m|\gamma_e|\eta_d^\top\eta$, it follows:

$$\dddot{\tilde{\xi}} = h - \frac{a_{11}}{m}\ddot{\tilde{\xi}} + |\gamma_e|\eta_d - |\gamma_e|(\eta_d^\top\eta)\eta$$
$$= h - \frac{a_{11}}{m}\ddot{\tilde{\xi}} + |\gamma_e|(\eta \times (\eta_d \times \eta))$$
$$= h - \frac{a_{11}}{m}\ddot{\tilde{\xi}} + \epsilon_1 \quad (26)$$

where $\epsilon_1 = |\gamma_e|(\eta \times (\eta_d \times \eta))$ is the additive perturbation term. It is shown in Pucci et al. (2015) that if $|\gamma| > m|\gamma_e|$ (for instance one can choose $\gamma = m|\gamma_e| + c$, with c any positive constant), we get $|\epsilon_1| < \frac{\sqrt{8V_1}}{m}$, therfore ϵ_1 converges to zero exponentially.

In case where $\epsilon_1 \equiv 0$, converse Lyapunov theorem ensures that there exists a quadratic Lyapunov function $V_2(\tilde{\xi}, \dot{\tilde{\xi}})$, such that in a neighborhood $(\tilde{\xi}, \dot{\tilde{\xi}}) = (0, 0)$, $\dot{V}_2 \leq -k_1V_2$. It follows that the function $V = \alpha V_1 + V_2$ is a Lyapunov function for the controlled system for $\alpha > 0$ large enough.

Adding integral action: To compensate for the large part of the wind and any other ignored slowly time-varying aerodynamic effects, an integral term should be added in the translational feedback control h. This term should be however bounded in order to avoid singularities in specifying the desired attitude. Among different possibilities, the bounded integrator I_p complemented with anti wind-up capabilities defined in Hua and Samson (2011) is chosen. It is the solution of the following differential equation (with $I_p(0) = \dot{I}_p(0) = 0$):

$$\ddot{I}_p = -k^{I1}\dot{I}_p + sat_{\frac{I_{p\max}^{(2)}}{2}}(k^{I2}(-I_p + sat_{\Delta^I}(I_p + \tilde{\xi})) \quad (27)$$

where k^{I1}, k^{I2}, Δ^I and $I_{p\max}^{(2)}$ are positive constants. It can be shown that $|I_p|$, $|\dot{I}_p|$, and $|\ddot{I}_p|$ are bounded respectively by $\delta^I + \frac{I_{p\max}^{(2)}}{2(k^{I1})^2}$, $\frac{I_{p\max}^{(2)}}{2k^{I1}}$ and $I_{p\max}^{(2)}$.

Defining the new variable $\tilde{\xi}_I = \tilde{\xi} + I_p$, recalling (19) and using the new arguments $\tilde{\xi}_I$ and $\dot{\tilde{\xi}}_I$ in the expression of h (22), we get:

$$\dddot{\tilde{\xi}}_I = h(\tilde{\xi}_I, \dot{\tilde{\xi}}_I) - \frac{a_{11}}{m}\ddot{\tilde{\xi}}_I + \gamma_e - \frac{1}{m}\bar{T}Re_3 + \ddot{I}_p + \frac{a_{11}}{m}\dot{I}_p$$
$$= h(\tilde{\xi}_I, \dot{\tilde{\xi}}_I) - \frac{a_{11}}{m}\ddot{\tilde{\xi}}_I + \gamma_e^I - \frac{1}{m}\bar{T}Re_3 \quad (28)$$

where $\gamma_e^I = \gamma_e + \ddot{I}_p + \frac{a_{11}}{m}\dot{I}_p$. The expressions of T_d and η_d are those given by (20) and (21) respectively, in which γ_e^I is used instead of γ_e. By applying the same attitude controller (23), we can show (with similar proofs to those proposed in Hua and Samson (2011)) the asymptotic stabilization of the equilibrium $(\tilde{\xi}, \dot{\tilde{\xi}}) = (0, 0)$ in case of a slowly time-varying perturbation term.

4. SIMULATION

In this section, a simulation example concerning a quadrotor performing the following Lissajous trajectory: $\xi_r(t) = (0.75\cos(t) - 0.75, 0.75\sin(t), 0.25\sin(2t))$, is analyzed. The idealized model (12)-(14) with $B = 0$, in which T and Ω are control inputs is at best an approximation of actual system dynamics. There are two main causes of errors for which the controller should be robust and

[1] The term $\frac{a_{11}}{m}\ddot{\tilde{\xi}}$ is so small that it can be ignored.

efficient: 1) a constant or slowly time-varying wind velocity, 2) the dynamic perturbation due to the presence of the flapping force part that depends on Ω ($B \neq 0$), resulting in direct coupling of the orientation dynamics with the translational dynamics. Two comparative results are presented: one concerns the controller developed in the paper and the other one concerns the classical control design case in which the flapping and induced drag are neglected. The effect of the integral action is also dealt with for both cases. The parameters of the system used for simulation are those identified by previous experiments (see for example Omari et al. (2013)) except for B which is believed to be negligible but here chosen comparable to A in order to analyze its effect: $m = 1.9Kg$, $g = 9.8m/s^2$, $\frac{a_{11}}{m} = 0.25$, $\frac{b_{12}}{m} = 0.6$. As for the control gains, the following choice has been made: $k_1(\eta, t) = \frac{K_1}{(1+\eta_d^T \eta)}$ with $K_1 = 5$, $k^p = 2$, $k^v = 2\sqrt{2}$, $k^{I1} = 0.5$, $k^{I2} = 0.1$, $\Delta^p = 2.5$, $\Delta^v = 2.5$, $\Delta^I = 0.175$, $I_{p_{max}}^{(2)} = 1.4$. As for the rotation dynamics, the following parameters are considered: $I = diag(0.0059, 0.0059, 0.0107)$, $d = 0.25$, $e = 0$, $c_T = 10^{-5}$, $c_Q = 10^{-6}$ and since the inertia matrix is small enough, the gain K_Ω is chosen equal to 0.17 and therefore $I^{-1}K_\Omega$ is large enough to ensure quick convergence of Ω to Ω_d. Finally and in order to simplify the control implementation $\gamma(t)$ has been ignored in the attitude controller (23). The initial conditions are $\xi(0) = (0.5, 0.5, -0.3)$, $\dot{\xi}(0) = \dot{\xi}_r(0) = (0, 0.75, 0.5)$ and $R(0) = I$ (horizontal attitude). In the first simulation the integral action is completely ignored. The controller given by (20) along with (22) and (23) is simulated in two different situations 1) as defined and 2) in case where we ignore the flapping and the induced drag ($a_{11} \equiv 0$) in the control while keeping it in the system's model. Note also that the modeling takes into account the forces created by each motor separately according to equation (10) that is without considering the approximate model around hovering.

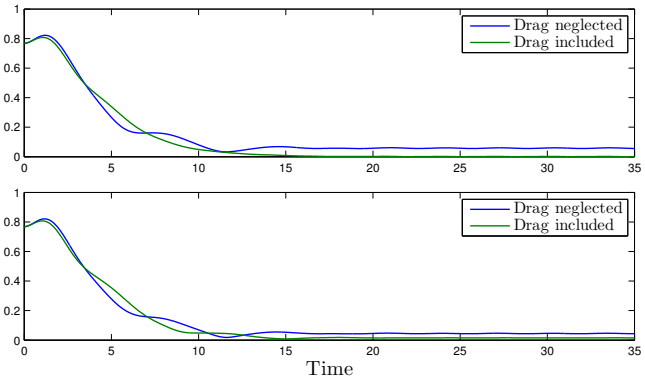

Fig. 6. Simulation results without integral action and without wind velocity: Position errors, $B = 0$ (upper plot) $B \neq 0$ (lower plot).

Figure 6 shows the superiority of the proposed controller w.r.t. the classical one in compensating for the perturbation caused by first-order drag forces without integral action. It also shows that when B is not negleted in the model, there is a small steady state error, however the term $\frac{b_{12}}{m} = 0.6$ is believed to be an exaggeration of the reality for small scale rotors according to other works on this topic (see for example Martin and Salaun (2010)). In the second simulation a wind velocity of $v_w = (1m/s, 1m/s, 0)$ has been added to the model, with the integral action still ignored. It is clear from figure 7 that the wind velocity

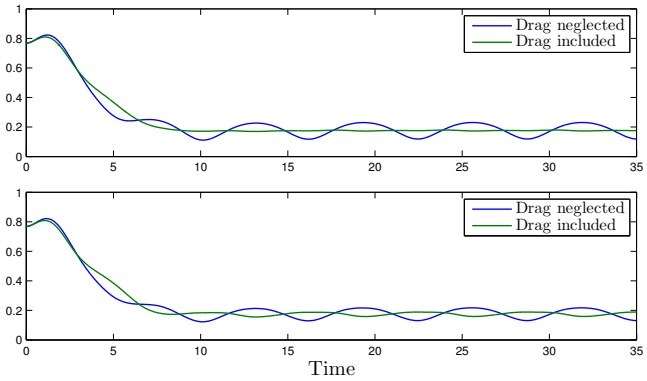

Fig. 7. Simulation results without integral action and with wind velocity: position errors, $B = 0$ (upper plot) $B \neq 0$ (lower plot).

causes a more important steady state error, it also induced oscillations with the classical controller that were canceled with drag augmented control. In the last simulation the integral action has been added as defined in equation (27) with the wind velocity maintained.

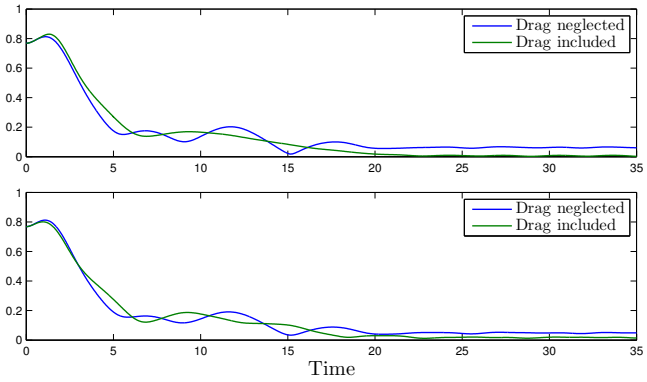

Fig. 8. Simulation results with integral action and with wind velocity: Position errors. $B = 0$ (upper plot) $B \neq 0$ (Lower plot).

Comparing figures 7 and 8, it is straightforward to verify the capability of the integral term in reducing partially the steady state error. This is not surprising given the practical importance of the integrator in refining the steady state response of the system. Note however that combining the integral action with a feedforward term that compensates for the flapping and induced drag forces is able not only to reduce the necessity of the slow integral action but even to cancel (or strongly reduce) the effect of these forces in the case where they are time varying as on accelerated trajectories. Note also that the term $\frac{b_{12}}{m}$ didn't show a significant impact on the response of the system.

In order to investigate further the capabilities of the control, we run a simulation on a more aggressive trajectory: $\xi_r(t) = (-\cos(t) + 1, 0.5\sin(2t), 0.25\sin(2t))$. This trajectory requires the quadrotor to deviate further from the hovering state, therefore it presents an opportunity

to predict the behavior of the vehicle in situations where the hypothesis taken in section 2.3 do not hold and where the simplified modeling of the first order drag forces may not be exact. We also choose a slowly varying wind vector (see Figure (10)) to support our discussion on the role of the integrator that should be able to deal with such perturbations. The values taken for the drag coefficients are the same as in the previous simulations.

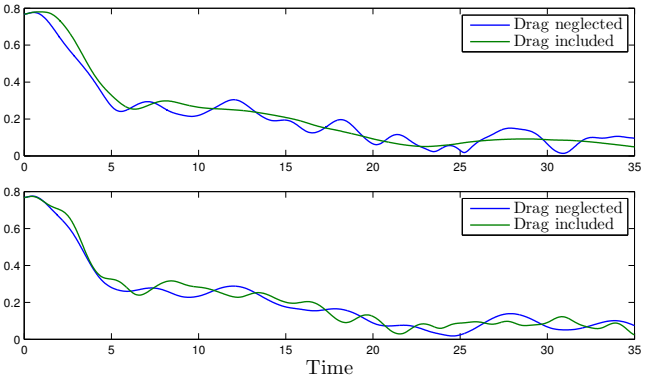

Fig. 9. Simulation results for an agressive trajectory with integral action and with slowly varying wind velocity: Position errors. $B = 0$ (upper plot) $B \neq 0$ (Lower plot).

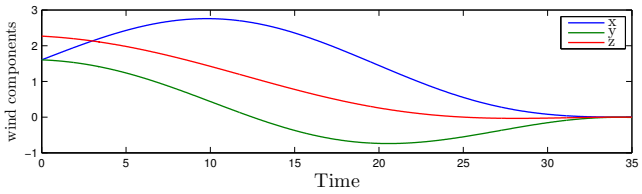

Fig. 10. Wind velocity components.

The results are shown in figure (9). For $B = 0$, one can clearly see that compensating for the first order drag forces keeps attenuating the oscillations of the vehicle's motion even with agressive maneuvers. But with $B \neq 0$, the flapping caused by the rotation motion generates significant zero dynamics that prevent us from giving a preference for a controller over the other, however as mentioned before the value $\frac{b_{12}}{m} = 0.6$ is an exagerration of the reality, therefore we expect the proposed control to have advantages over the classical control in practice.

5. CONCLUSION

A mathematical model of propeller aerodynamics has been derived and applied to the case of a quadrotor, which predicts the existence of first order linear drag around hovering. We investigated both cases of rigid and flexible rotors and found that drag forces are more preponderant in the latter case, but with the advantage of eliminating gyroscopic torques. A design of position control taking these forces into account has been proposed. We have shown that the drag forces resulting from linear velocity can be exploited in control design, whereas those resulting from angular velocity in the case of flexible rotors can be neglected. The proposed position control has been validated by simulation, showing that including drag forces in the controller clearly improves the position tracking performance.

ACKNOWLEDGEMENTS

This research was supported by the French *Agence Nationale de la Recherche* via the ROBOTEX project (ANR-10-EQPX-44). The authors would like to thank Prof. Claude Samson for his help and valuable discussions.

REFERENCES

Bangura, M. and Mahony, R. (2012). Nonlinear dynamic modeling for high performance control of a quadrotor. In *Proc. Australasian Conf. Robotics Automation*, 3–5.

Bangura, M., Melega, M., Naldi, R., and Mahony, R. (2016). Aerodynamics of rotor blades for quadrotors. *arXiv preprint arXiv:1601.00733*.

Bramwell, A. (2001). *Helicopter Dynamics*. George Done and David Balmford.

Bristeau, P.J., Martin, P., Salaün, E., and Petit, N. (2009). The role of propeller aerodynamics in the model of a quadrotor uav. In *European Control Conference (ECC)*, 683–688.

Hamel, T., Mahony, R., Lozano, R., and Ostrowski, J. (2002). Dynamic modelling and configuration stabilization for an x4-flyer. In *15th IFAC World Congress*, 217–222.

Hua, M.D., Hamel, T., Morin, P., and Samson, C. (2013). Introduction to Feedback Control of Underactuated VTOL Vehicles. *IEEE Control Systems Magazine*, 33(1), 61–75.

Hua, M.D. and Samson, C. (2011). Time sub-optimal nonlinear PI and PID controllers applied to Longitudinal Headway Car Control. *Int. Journal of Control*, 84(10), 1717–1728.

Mahony, R., Kumar, V., and Corke, P. (2012). Multirotor aerial vehicles: Modeling, estimation, and control of quadrotor. *IEEE Robot. Automat. Mag.*, 19(3), 20–32.

Martin, P. and Salaun, E. (2010). The true role of accelerometer feedback in quadrotor control. In *IEEE International Conference on Robotics and Automation (ICRA)*, 1623–1629.

Omari, S., Hua, M.D., Ducard, G., and Hamel, T. (2013). Nonlinear control of vtol uavs incorporating flapping dynamics. In *2013 IEEE/RSJ International Conference on Intelligent Robots and Systems*, 2419–2425.

Plessis, J.D. and Pounds, P. (2014). Rotor flapping for a triangular quadrotor. In *Proc. Australasian Conference on Robotics and Automation*.

Pounds, P. (2007). *Design construcion and control of a large quadrotor micro air vehicle*. Ph.D. thesis, Australian National University.

Pounds, P., Mahony, R., and Corke, P. (2010). Modelling and control of a large quadrotor robot. *Control Engineering Practice, Special Issue on Aerial Robotics*, 18(7), 691 – 699.

Prouty, R. (2002). *Helicopter Performance, Stability, and Control*. first ed. Krieger Publishing Company.

Pucci, D., Hamel, T., Morin, P., and Samson, C. (2015). Nonlinear feedback control of axisymmetric aerial vehicles. *Automatica*, 53, 72–78.